

## **Supporting Information**

# **Surface Passivation of Organic-Inorganic Hybrid Perovskites with Methylhydrazine Iodide for Enhanced Photovoltaic Device Performance**

**Chongzhu Hu<sup>1,2,3,4</sup>, Zhuangzhuang Zhang<sup>2,3,4</sup>, Jun Chen<sup>1,\*</sup> and Peng Gao<sup>2,3,4,\*</sup>**

<sup>1</sup> Faculty of Materials Metallurgy and Chemistry, Jiangxi University of Sciences and Technology, Ganzhou 341000, China

<sup>2</sup> CAS Key Laboratory of Design and Assembly of Functional Nanostructures Fujian Institute of Research on the Structure of Matter Chinese Academy of Sciences Fuzhou, Fujian 350002, P. R. China

<sup>3</sup> Xiamen Key Laboratory of Rare Earth Photoelectric Functional Materials, Chinese Academy of Science, Xiamen 361021, Fujian, People's Republic of China

<sup>4</sup> Laboratory for Advanced Functional Materials, Xiamen Institute of Rare Earth Materials, Haixi Institute, Chinese Academy of Sciences, Xiamen 361021, P. R. China

\* Correspondence: chenjun@jxust.edu.cn (J.C.); peng.gao@fjirsm.ac.cn (P.G.);

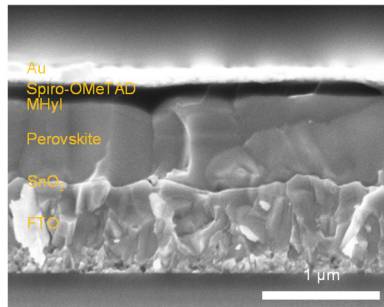


**Figure S1.** Cross-sectional SEM image of target device.

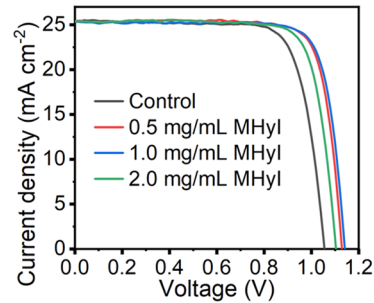


**Figure S2.**  $J$ – $V$  curves of the PSCs treated with different concentrations of MHyl solution.

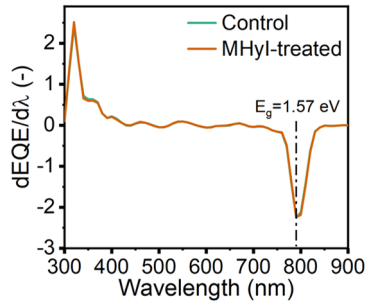


**Figure S3.** Determination of the absorption of the perovskite absorber by the differential of EQE curves.

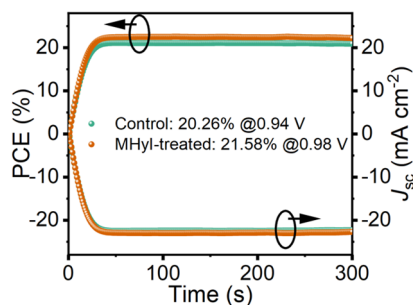


**Figure S4.** The SPO of the control and MHyl-treated devices.

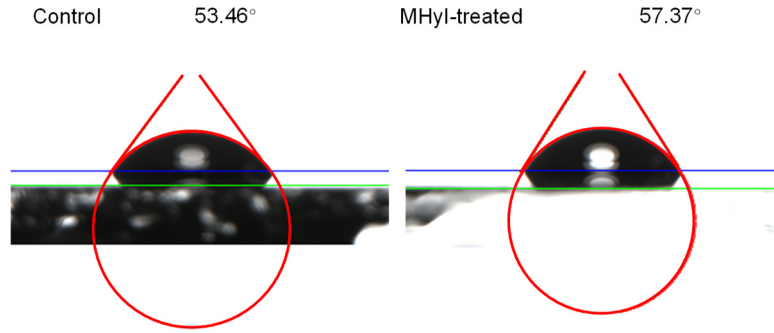


**Figure S5.** The static water contacts angle of the standard film and MHyl-treated film.

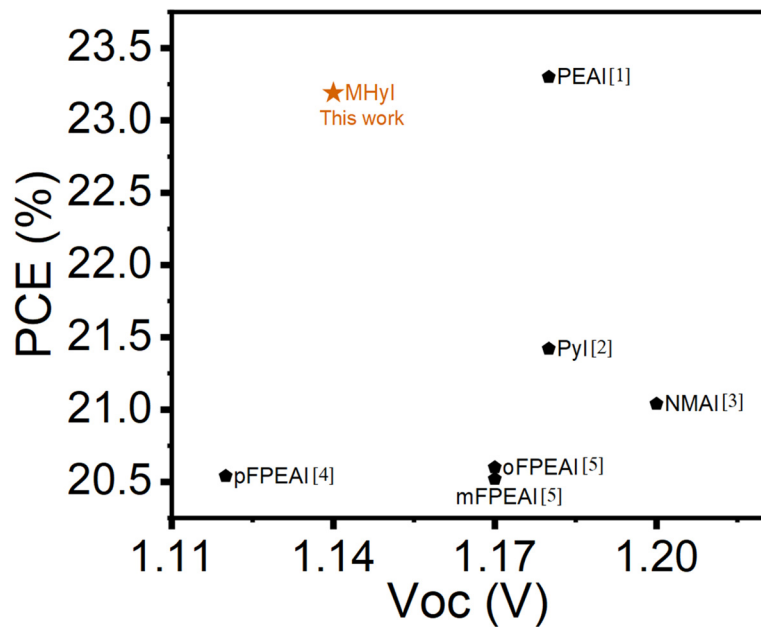


**Figure S6.** Comparative performance of devices with different post-treatment ammonium salts (PEAI [1], PyI [2], NMAI [3], pFPEAI [4], oFPEAI [5], mFPEAI [5]).

**Table S1.** Fitted results of TRPL curves of perovskite films with and without MHyl-modified and average PL lifetime  $\tau_{ave}$  was calculated using  $\tau_{ave} = (A_1\tau_1^2 + A_2\tau_2^2) / (A_1\tau_1 + A_2\tau_2)$ .

	A <sub>1</sub>	$\tau_1$ (ns)	A <sub>2</sub>	$\tau_2$ (ns)	$\tau_{ave}$ (ns)
Control	0.36	31.67	0.57	131.53	118.09
MHyl-treated	0.19	35.46	0.73	354.56	346.37

**Table S2.** Fitting parameters of the EIS measurement based on control and MHyl-treated perovskite solar cells.

	R <sub>s</sub> ( $\Omega$ )	C <sub>tr</sub> (F)	R <sub>tr</sub> ( $\Omega$ )	C <sub>rec</sub> (F)	R <sub>rec</sub> ( $\Omega$ )
Control	10.90	$2.115 \times 10^{-6}$	$1.125 \times 10^5$	$1.092 \times 10^{-8}$	$2.189 \times 10^4$
MHyl-treated	10.16	$1.796 \times 10^{-6}$	$1.504 \times 10^5$	$1.101 \times 10^{-8}$	$3.932 \times 10^4$

**References:**

1. Jiang, Q.; Zhao, Y.; Zhang, X.; Yang, X.; Chen, Y.; Chu, Z.; Ye, Q.; Li, X.; Yin, Z.; You, J. Surface Passivation of Perovskite Film for Efficient Solar Cells. *Nature Photonics* **2019**, *13*, 460–466, doi:10.1038/s41566-019-0398-2.
2. Du, Y.; Wu, J.; Zhang, X.; Zhu, Q.; Zhang, M.; Liu, X.; Zou, Y.; Wang, S.; Sun, W. Surface Passivation Using Pyridinium Iodide for Highly Efficient Planar Perovskite Solar Cells. *Journal of Energy Chemistry* **2021**, *52*, 84–91, doi:10.1016/j.jecchem.2020.04.049.
3. Liang, L.; Luo, H.; Hu, J.; Li, H.; Gao, P. Efficient Perovskite Solar Cells by Reducing Interface-Mediated Recombination: A Bulky Amine Approach. *Advanced Energy Materials* **2020**, *10*, doi:10.1002/aenm.202000197.
4. Zhou, Q.; Liang, L.; Hu, J.; Cao, B.; Yang, L.; Wu, T.; Li, X.; Zhang, B.; Gao, P. High-Performance Perovskite Solar Cells with Enhanced Environmental Stability Based on a (p-FC 6 H 4 C 2 H 4 NH 3 ) 2 [PbI 4 ] Capping Layer. *Advanced Energy Materials* **2019**, *9*, doi:10.1002/aenm.201802595.
5. Zhou, Q.; Xiong, Q.; Zhang, Z.; Hu, J.; Lin, F.; Liang, L.; Wu, T.; Wang, X.; Wu, J.; Zhang, B.; et al. Fluoroaromatic Cation-Assisted Planar Junction Perovskite Solar Cells with Improved VOC and Stability: The Role of Fluorination Position. *Solar RRL* **2020**, *4*, doi:10.1002/solr.202000107.